VIRTUAL MODEL OF THE UCSD-NEES HIGH PERFORMANCE OUTDOOR SHAKE TABLE

O. Ozcelik, J. P. Conte, and J. E. Luco

University of California, San Diego, CA 92093 USA

oozcelik@ucsd.edu, jpconte@ucsd.edu, jeluco@ucsd.edu

Abstract

In this study an early version of a virtual model of the UCSD-NEES shake table is presented. This virtual model includes the following subsystems: a virtual replica of the controller, nonlinear servo-valve model, single-ended actuator model with internal volume change, and simplified models of the mechanical subsystems, namely a rigid platen, horizontal stiffness provided by the hold-down struts, and dissipative/friction force mechanisms. Comparison of actual test data and simulation data show that this model, with the same controller gains as those used on the real system, is able to reproduce the signal distortion observed in sinusoidal test data. Improvements in the virtual model are needed for reproducing the actual system response to commanded broadband signals such as earthquake records. A more advanced version of this virtual model will be used to improve the performance of the current controller based on physical knowledge of the shake table system.

Introduction

Large servo-hydraulic shaking table systems are essential tools in experimental earthquake engineering. They provide effective ways to subject specimens of structural components, substructures, or entire structural systems to dynamic excitations similar to those induced by real earthquakes. Within the NEES Consortium, major shake table facilities exist at Buffalo, Reno, and San Diego. The UCSD-NEES Large High Performance Outdoor Shake Table (LHPOST) at Camp Elliott enables landmark seismic experiments to be conducted on large- and full-scale structural and soil-foundation-structure interaction systems. The specifications for the LHPOST are a stroke of ±0.75m, a peak horizontal velocity of 1.8m/s, a horizontal force capacity of 6.8MN, an overturning moment capacity of 50MN-m, and a vertical payload capacity of 20MN. The frequency bandwidth is 0-20Hz. The LHPOST consists of a moving steel platen (7.6m wide by 12.2m long), a reinforced concrete reaction block, two servo-controlled dynamic actuators with a force capacity in tension/compression of 2.7MN and 4.2MN, respectively, a platen sliding system (6 hydrostatic pressure balanced bearings each with a vertical force capacity of 9.4MN), an overturning moment restraint system consisting of two nitrogen-filled hold-down struts, a yaw restraint system (two hydrostatic pressure balanced bearings on each longitudinal side of the platen), a real-time multi-variable controller, and a hydraulic power supply system.

The complex dynamics of large shaking table systems emanate from multiple dynamic interactions and nonlinearities among various system components. An interaction diagram of the subsystems of the LHPOST is shown in Figure 1.

Due to concerns about prematurely damaging the specimen, the tuning of current shaking table controllers is typically conducted at a scaled down version of the target ground motion or under bare table condition. As a result of the complexity of the complete table-specimen system, controller tuning at scaled down amplitudes leads to significant errors when the full-scale input is commanded as shown by recent experiments performed on the UCSD-NEES table. Thus, there is a crucial need to improve the controller based on physical knowledge of the system. This can be done, as a first step, by developing a comprehensive mechanics-based model of the system. This model will also
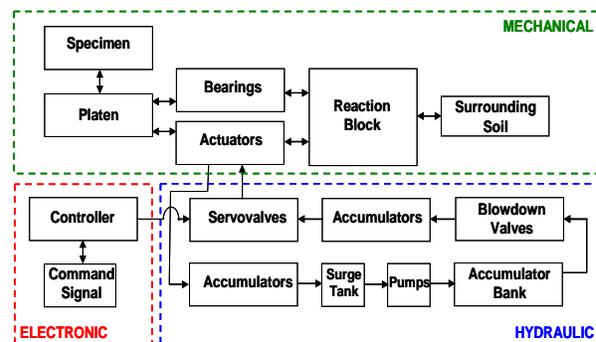

Figure 1. Component and interaction diagram of shake table system

play a critical role in planning and designing shake table experiments, optimizing the location of sensors, interpreting the results of experiments, and off-line virtual tuning of the actual controller using the system simulation model.

A complete virtual model of the LHPOST would require the following components (Figure 1) to be modeled: reaction block and surrounding soil, platen and supporting bearings, actuators, servo-valves, accumulators, hydraulic pumps, controller, and test specimens. Since shake table experiments are often performed to investigate the nonlinear behavior of structural systems under strong earthquake excitation, nonlinear finite element models of structural specimens must be incorporated in the virtual system model.

In the literature, we find a limited number of studies focusing on modeling and simulation of complete shake table systems (Hwang et al., 1987; Rinawi and Clough, 1991; Clark, 1992; Conte and Trombetti, 2000; Trombetti and Conte, 2002; Twitchell and Symans, 2003). In particular, Conte and Trombetti (2000) developed a linear analytical model of a small-to-medium size shake table system accounting for servovalve time delay, actuator dynamics, oil leakage through the actuator seals, foundation flexibility, and linear elastic multi-degree-of-freedom (MDOF) specimen dynamics. Williams et al. (2001) have developed a realistic model of a dynamic structural testing system, which includes a detailed nonlinear model of the servovalve actuator system, the controller, and the specimen modeled as a linear elastic single-degree-of-freedom (SDOF) system.

A comprehensive virtual model of the LHPOST with all the components shown in Figure 1 is under development. In this paper, an early version of this virtual UCSD-NEES shake table model is presented. The components of the LHPOST incorporated in the current model consist of: the control algorithm (a virtual replica of the actual controller), four servo-valves, two single ended actuators, nitrogen-filled hold-down struts, various dissipative and friction mechanisms existing in the system, and the platen. Actual physical quantities identified for this virtual model through tests conducted on the system are the effective mass of the platen, effective horizontal stiffness provided by the hold-down struts, and effective dissipative/friction forces. Comparisons between actual system response and its prediction obtained through the current virtual model are provided for harmonic tests.

Formulation and Implementation of the Components of the Virtual Shake Table Model

This section presents some of the mathematical formulations of the various components of the virtual model of the overall shake table system and their implementations in the Matlab-Simulink programming environment.

Controller

The controller of the LHPOST consists of MTS digital Three Variable Controller (TVC) referred to as Model 469DU and known in control theory as a state variable controller. It has additional special features to compensate for linear and nonlinear system distortions for both harmonic and broadband command signals (e.g., amplitude/phase control, adaptive harmonic cancellation, adaptive inverse control, on-line iteration, and notch filters). The three state variables controlled by the TVC are displacement, velocity, and acceleration. The controller can be set to run under displacement, velocity or acceleration control mode. Depending on the control mode, only one state variable becomes the primary control variable with the others serving only as compensation (feed-forward and/or feedback) signals to improve damping and stability of the system. The transfer functions between all the inputs and outputs of the TVC were provided by MTS Systems Corporation. Details regarding these transfer functions and their implementation in Matlab-Simulink can be found elsewhere (Thoen, 2004).

A conceptual representation of the controller is given in Figure 2. The reference generator takes the reference signal, which represents the desired displacement, velocity, or acceleration depending on the control mode, and creates the reference states x_{ref}, $\dot{x}_{ref}$, $\ddot{x}_{ref}$, and $\dddot{x}_{ref}$ (jerk), which are used as feed-

forward signals in the controller. The feedback states x_{fbk}, $\dot{x}_{fbk}$, and $\ddot{x}_{fbk}$ are generated by the feedback generator which combines displacement and acceleration sensors (feedback signals), each with their respective bandwidth limitations to create wideband estimates of the feedback states. The reference and feedback states are weighted by the reference and feedback gains, respectively, shown in the figure. It should be noted here that the displacement feedback gain is the only non-zero feedback gain. Therefore, it can be said that the TVC is simply a displacement controller with sophisticated reference (feed-forward) gains (Thoen, 2001). The high-pass filter applied on the force feedback signal (equivalent to the delta-pressure signal multiplied by the actuator effective piston area) removes static and low frequency components from the force feedback, prior to input it into the TVC to damp the oil column resonance. Five notch filters are also incorporated in the controller to compensate for resonances and anti-resonances. Each notch filter frequency response is defined by three parameters: the center frequency, 3dB bandwidth, and notch depth (Thoen, 2004).
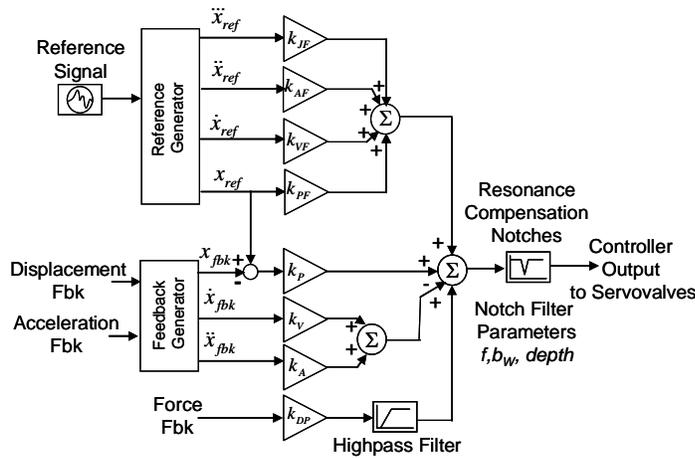

Figure 2. Conceptual representation of TVC.

Note that signals with different units are blended together. Blending of signals with different units to obtain a hybrid command signal to the servo-valves is possible through normalization of the various signals to their respective maximum value (e.g., D_{max}, V_{max}, A_{max}, F_{max}) and conversion to Volt units (not shown in the figure).

Servo-Valves

There are four four-stage servo-valves in the system, two at each actuator. These servo-valves are specially manufactured to achieve the high performance specifications of the LHPOST. The fourth stage flow rating of each servo-valve is 10,000 lit/min.

Servo-valves are inherently nonlinear devices in which the flow output is proportional to the square root of the pressure drop across them. An overall schematic of servo-valve and actuator combination with four flow paths corresponding to the extent and retract directions of the actuator piston is shown in Figure 2.
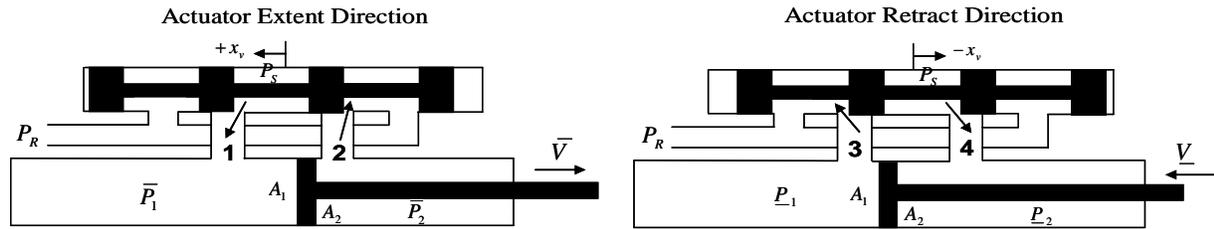

Figure 3. Four stage servovalve and single ended actuator combination with four flow paths ($\overline{V}$ and $\underline{V}$ are the extent and retract velocities of the actuator piston, respectively).

The four flows from the servovalve orifices (labeled 1 through 4) into the actuator chambers can be expressed using Bernoulli's equation as

$$q_1 = A_1\overline{V} = K_v w_1 x_{sv}\sqrt{P_S - \overline{P}_1} \qquad\qquad q_3 = A_1\underline{V} = K_v w_3 x_{sv}\sqrt{\underline{P}_1 - P_R} \qquad (1)$$

$$q_2 = A_2\overline{V} = K_v w_2 x_{sv}\sqrt{\overline{P}_2 - P_R} \qquad\qquad q_4 = A_2\underline{V} = K_v w_4 x_{sv}\sqrt{P_S - \underline{P}_2} \qquad (2)$$

where A_1 and A_2 are the compression and tension areas of the actuator piston, respectively; K_v is a linearized flow coefficient; x_{sv} is the servovalve 4th stage spool displacement; w_1, w_2, w_3, w_4 are the specially manufactured valve port window widths; and P_S and P_R denote the system supply pressure and the return pressure, respectively ($P_S \cong 20.7$ MPa and $P_R \cong 0.35$ MPa).

Due to the single ended nature of the actuators, the actuator piston areas on the tension and the compression sides are different; the ratio of tension area ($0.1297 \, \text{m}^2$) to compression area ($0.2027 \, \text{m}^2$) is 0.64 for both actuators. A design criterion for achieving minimum waveform distortion for single ended actuators is to keep the no load (i.e., zero force carried by the actuator) pressures within the actuator the same for each direction of travel while maintaining the same constant velocity. With this criterion satisfied, there is theoretically no pressure discontinuity in each chamber when the actuator piston changes direction (Gram, MTS Systems Corporation, personal communication, 2006). This criterion reduces to the following conditions on the port orifice widths:

$$\frac{w_1}{w_3} = \left(\frac{A_2}{A_1}\right)^{1/2} = 0.8, \quad \frac{w_2}{w_3} = \left(\frac{A_2}{A_1}\right)^{3/2} = 0.512, \quad \frac{w_3}{w_3} = 1, \quad \frac{w_4}{w_3} = \frac{A_2}{A_1} = 0.64 \qquad (3)$$

Once the fourth stage spool displacement, x_{sv}, of a servo-valve is known, the corresponding port orifice areas can be obtained as the product of x_{sv} and port orifice width as given in (3) where $w_3 = 25.4$ cm. Then, by using these port orifice areas, the flows from servo-valves into actuator chambers can be found from (1) and (2) for given values of P_1 and P_2.

The servovalve spool displacement (inner) control loop within the servovalve exhibits second-order low-pass dynamics. These dynamics can be measured by exciting the table with a random command signal, recording valve driver command and valve spool displacement feedback, and fitting an Auto Regressive Moving Average (ARMA) dynamic model to the data (Williams et al., 2001; Thoen and Laplace, 2004). Modeling of the fourth stage servo-valve spool dynamics is not included herein due to lack of the needed experimental data. Only a simple conversion factor is used to convert the valve command signal in Volts to the servo-valve spool displacement in mm (19.05/10 mm/V). Once the necessary data is available, the spool dynamics will be incorporated in the shake table simulation model.
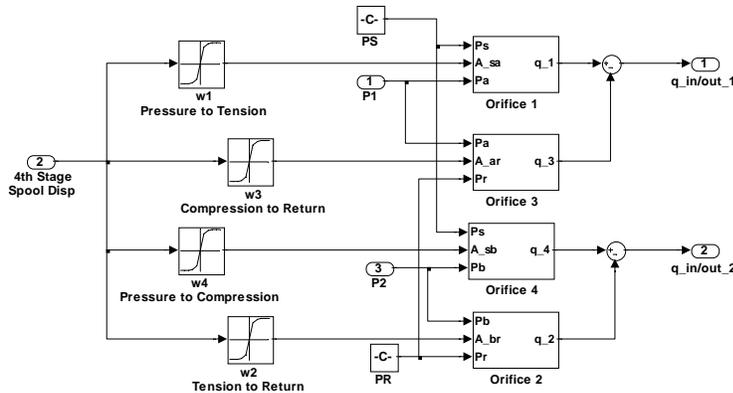

Figure 4. Matlab-Simulink implementation of a four-way servovalve.

The Matlab-Simulink implementation of the fourth stage of a four-way servo-valve with the above mentioned characteristics is given in Figure 4. Herein, four-way defines the number of flow paths in and out of the servovalve. The orifice 1 to 4 sub-blocks contain the implementation of Bernoulli's equations given in (1) and (2) to compute the flows into the actuator chambers, while the w_1 to w_4 sub-blocks calculate the port orifice areas as a function of the fourth stage spool displacement, x_{sv}. Since the LHPOST has four four-way servo-valves, four servo-valve models as shown in Figure 4 are implemented in the virtual shake table model.

Single Ended Actuators

The servo-valve model developed in the previous section determines the oil flow into the actuator pressure chambers. The load pressure (differential pressure across the actuator piston) that drives the actuator piston can be derived from the flow continuity equation. The actuator model used in this study takes into account the change in volume of the actuator chambers (Williams et al., 2001), a source of nonlinearity. Each single-ended actuator has two pressure chambers as shown in Figure 5.

By integrating in time the equation of flow continuity, the expressions for the actuator chamber pressures P_1 and P_2 can be obtained as

$$P_1 = \int \frac{\left(q_1 - A_1 \dfrac{dy}{dt}\right)\beta y_{stroke}}{\overline{v}_1\left(y_{stroke} + y\right)} dt \; , \qquad P_2 = -\int \frac{\left(q_2 - A_2 \dfrac{dy}{dt}\right)\beta y_{stroke}}{\overline{v}_2\left(y_{stroke} - y\right)} dt \qquad (4)$$

where A_1 and A_2 are the piston areas, $y(t)$ is the piston displacement relative to the actuator cylinder (which is equal to the platen total displacement assuming that the platen, actuators, reaction block and surrounding soil are all rigid), P_1 and P_2 are the actuator chamber pressures, β is the oil bulk modulus ($\beta = 689.5$ MPa from the literature), and $\overline{v}_1$ and $\overline{v}_2$ are the initial actuator chamber volumes. Once the actuator chamber pressures are known, the actuator driving force can be obtained as $F_{act}(t) = P_1 A_1 - P_2 A_2$.
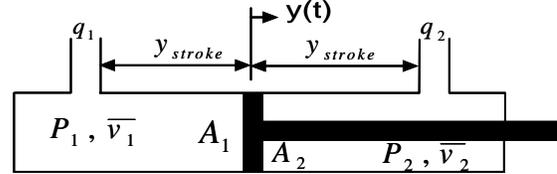

Figure 5. Single-ended actuator with actuator piston at the centered position.

The Matlab-Simulink implementation of the single-ended actuator model defined above with varying chamber volumes is shown in Figure 6. Since the LHPOST has two single-ended actuators, two actuator models as shown in Figure 6 are implemented in the virtual shake table model.
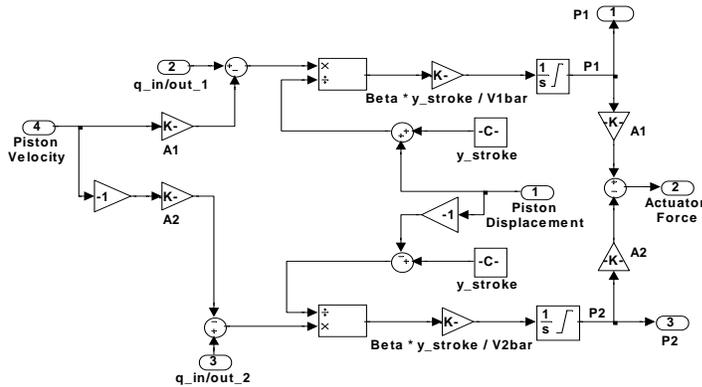
Modeling and Identification of Mechanical Subsystems

The mechanical components of the LHPOST considered in this paper include a moving steel platen, a platen sliding system composed of six hydrostatic pressure balanced bearings, a yaw restraint system with two hydrostatic pressure balanced bearings on each longitudinal side of the platen, and an overturning moment restraint system provided by a discrete tension cylinder pre-stressing system consisting of two nitrogen-filled hold-down struts.

Figure 6. Matlab-Simulink implementation of the single-ended actuator model.

For identification purposes, a simplified mathematical model with a small number of parameters of the above mentioned mechanical components of the LHPOST needs to be defined. Such a model is given in Figure 7, where $F_{act}(t)$ is the total actuator force applied to the table by the two horizontal actuators, M_e is the effective mass of the platen, K_e is the total effective horizontal stiffness provided by the two hold-down struts, C_e is the effective viscous damping coefficient, and μ_e is the effective Coulomb friction

force, and $u_x(t)$ is the horizontal movement of the platen along x direction. The rationale behind choosing these parameters to model the mechanical system can be found elsewhere (Ozcelik et al., 2006).

The equation of motion of the conceptual model given in Figure 7 can be written as follows

$$M_e \ddot{u}_x(t) + K_e u_x(t) + \left(C_e \left| \dot{u}_x(t) \right|^\alpha + \mu_e \right) sign(\dot{u}_x(t)) = F_{act}(t) \tag{5}$$
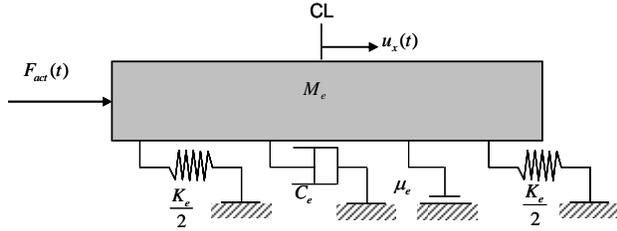

Figure 7. Conceptual mathematical model of the mechanical subsystems of the LHPOST

The unknown parameters of the above model were estimated by using an extensive set of tests performed on the system ranging from simple harmonic tests to earthquake and white noise tests. Details regarding the estimation procedure can be found in Ozcelik et al. (2006). The estimated model parameters are $M_e = 144$ tons, $K_e = 1.266\,\text{MN/m}$, $C_e = 0.041\,\text{MN-s/m}$, $\alpha = 0.5$, and $\mu_e = (0.538\%) \cdot F_V$. The dissipative force term appearing in (5) is a function of velocity. In order to take this variation into account, the following viscoplastic friction law is used (Bondonet et al., 1997):

$$F_H = \left(C_e \left| \dot{u}_x(t) \right|^\alpha + \mu_e \right) Z , \qquad Y \frac{dZ}{dt} = \left\{ 1 - Z^2 \left[\kappa + \left(1 - \kappa \right) sign\left(Z \dot{y} \right) \right] \right\} \dot{y} \tag{6}$$

where F_H is the effective horizontal dissipative force, Z is the hysteretic dimensionless parameter which satisfies (6)₂, Y is the equivalent yield displacement, and κ is a dimensionless constant. The values of Y and κ used in this study are 0.2 mm and 0.5, respectively. The Matlab-Simulink implementation of the above dissipative force model is shown in Figure 8.
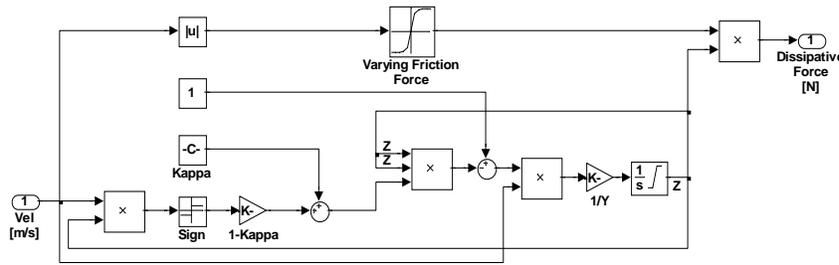

Figure 8. Matlab-Simulink implementation of the viscoplastic friction law.

Notice that the "Varying Friction Force" block shown in Figure 8 implements the dissipative force given in (6)₁.

The Simulink implementation of the rigid platen and the horizontal stiffness due to the pre-charged hold-down struts is not given here due to space limitation.

Virtual Model of Shake Table System and Comparison of Experimental and Simulation Results

The Matlab-Simulink implementation of the complete virtual model of the LHPOST is shown in Figure 9. Notice the modular implementation of the various subsystems, which enhances the understanding of the interaction between the various components and sub-systems.

Data obtained from sinusoidal tests performed on the real system under bare table conditions (no specimen attached to the platen) are used to assess the prediction capability of the virtual model. Test data obtained from two sine tests both at 3 Hz frequency and 1.73g (SP07) and 3.20g (SP09) target amplitude were used for comparison purposes. The control gains for these tests were set at: displacement gain = 1.5 (V/V) (the only nonzero feedback gain), displacement lead = 0.0 (V/V), velocity lead = 0.38 (V/V),

acceleration lead = 0.52 (V/V), jerk lead = 0.005 (V/V), and dynamic force gain = -1.5 (V/V). These same control gain values are used in the virtual model of the LHPOST.
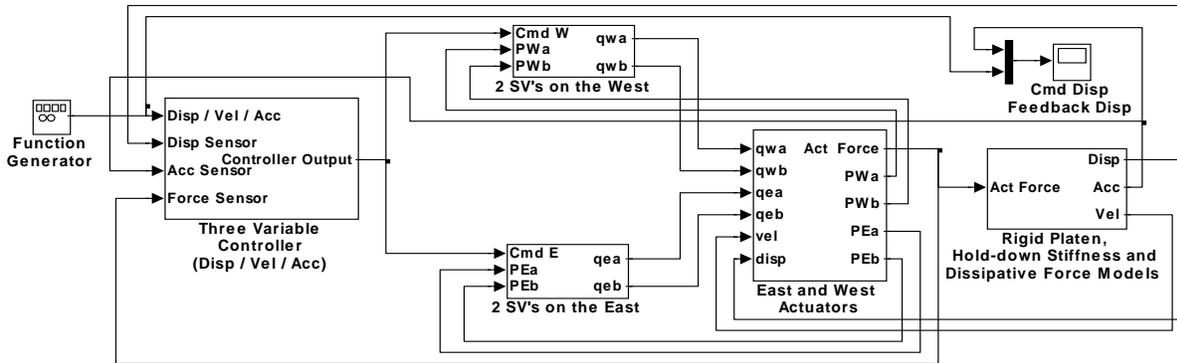

Figure 9. Complete virtual model of the LHPOST (under bare table condition).

Comparison of feedback platen accelerations obtained from the actual tests and the simulation model is given in Figure 10. It is observed that the actual and simulated feedback acceleration records are in good agreement. The prediction accuracy of the virtual model decreases as the amplitude of the reference increases. One possible explanation for this discrepancy is that the servo-valve model used, Equations (1) and (2), does not take into account the nonlinear relationship between servo-valve spool displacement and servo-valve flow (Zhao et al., 2005). Nevertheless the simulation model is able to capture the distortion seen in the actual feedback acceleration records. It was found that odd harmonics of the fundamental frequency cause this distortion in the feedback signal and that the mechanical source of this distortion is the nonlinearity in the servo-valve orifice flow. Simulations based on a linear servo-valve model for which the flow into the actuator is

Figure 10.Test-Analysis Comparison.

calculated simply by multiplying the spool displacement with a certain flow gain (obtained from the manufacturer) do not capture the odd-harmonic distortion observed in the actual feedback signal.
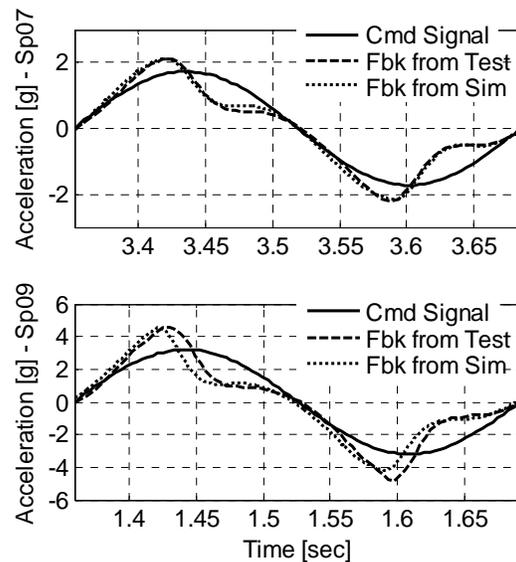
Conclusions

In this study, an early version of the virtual model of the UCSD-NEES large high-performance outdoor shake table is presented. This model incorporates a virtual replica of the actual controller, nonlinear models of servo-valves with specially manufactured port orifice widths, single-ended actuator models with variable internal volume change, and simplified models of mechanical sub-systems including rigid platen, horizontal stiffness provided by the hold-down struts, and dissipative force mechanisms modeled through a combination of Coulomb friction and viscous damping forces.

Comparison of actual recorded test data with simulation data shows that the current version of the virtual model with the same controller gains as on the actual system is able to capture the main features of the actual sinusoidal test data. It was found that the distortion seen in the actual feedback signals is due to the nonlinearity in the servo-valve orifice flow. Comparisons (not shown herein) of actual and simulated data

for broadband command signals (white noise and earthquake records) do not show as good an agreement as that observed for the sinusoidal tests. Future improved versions of the virtual shake table model will incorporate the flexibility of the platen, the reaction block and the surrounding soil, detailed models of the supporting vertical and lateral bearings, the dynamics of the 3rd and 4th stage spools of the servo-valves, the nonlinear relationship between servo-valve spool displacement and servo-valve flow, and finally internal and external leakage in the actuators and servo-valves. Nonlinear models of typical test specimens will also be developed and integrated into the shake table virtual model to study the shake table - specimen interaction. This improved comprehensive mechanics based virtual model will then be used as a starting point to improve the existing controller based on physical knowledge of the system.

References

Bondonet, G. and A. Filiatrault (1997), "Frictional Response of PTFE Sliding Bearings at High Frequencies," *Journal of Bridge Engineering, ASCE*, **2**(4), 139-148.

Clark, A. (1992), "Dynamic Characteristics of Large Multiple Degree of Freedom Shaking Tables," *Proc. 10th World Conf. on Earthquake Engineering*, Madrid, Spain, 2823-2828.

Conte, J.P. and T.L. Trombetti (2000), Linear Dynamic Modeling of a Uni-axial Servo-Hydraulic Shaking Table System," Earthquake Engineering and Structural Dynamics, 29, 1375-1404.

Hwang, J. S., K.C. Chang, and G.C. Lee (1987), "The System Characteristics and Performance of a Shaking Table," NCEER Report No. 87-0004, National Center for Earthquake Engineering Research, State University of New York at Buffalo, NY, 1987.

McKenna, F. and G.L. Fenves (2000), "An Object-Oriented Software Design for Parallel Structural Analysis," *Proc. of the SEI/ASCE Structures Congress*, Philadelphia, PA, 2000.

Ozcelik, O., J.E. Luco, J.P. Conte, and T.L. Trombetti (2006), "Experimental Characterization, Modeling and Identification of the Mechanical Subsystem of the UCSD-NEES Shake Table," in preparation, 2006.

Rinawi, A. M., and R.W. Clough (1991), "Shaking Table-Structure Interaction," EERC Report No. 91/13, Earthquake Engineering Research Center, University of California at Berkeley, CA, 1991.

Thoen, B. K. (2001), "How to Tune Three Variable Controller (TVC)", MTS Corporation, 2001.

Thoen, B. K. (2004), "TVC Transfer Functions", MTS Corporation, 2004.

Thoen, B. K., and P.N. Laplace (2004), "Offline Tuning of Shaking Tables," *Proc. 13th World Conf. on Earthquake Engineering, Vancouver, B.C.*, Canada, Aug. 1-6, Paper No. 960, 2004.

Trombetti, T.L. and J.P. Conte (2002), "Shaking Table Dynamics: Results from a Test Analysis Comparison Study," *Journal of Earthquake Engineering*, **6**(4), 513-551.

Twitchell, B. S. and M.D. Symans (2003), "Analytical Modeling, System Identification, and Tracking Performance of Uniaxial Seismic Simulators," *Journal of Engineering Mechanics*, **129**(12), 1485-1488.

Williams, D. M., M.S. Williams and A. Blakeborough (2001), "Numerical Modeling of a Servohydraulic Testing System for Structures," *Journal of Engineering Mechanics*, **127**(8), 816-827.

Zhao, J., C. Shield, C. French and T. Posbergh (2005), "Nonlinear System Modeling and Velocity Feedback Compensation for Effective Force Testing," *Journal of Engineering Mechanics*, 131(3), 244-253.